

5 KINEROS2 and the AGWA modelling framework

D. J. Semmens, D. C. Goodrich, C. L. Unkrich, R. E. Smith, D. A. Woolhiser, and S. N. Miller

5.1 INTRODUCTION

This chapter describes the conceptual model, mathematical model, and numerical methods underpinning the Kinematic Runoff and Erosion Model, KINEROS2. The performance of KINEROS2 and its numerous components has been evaluated in numerous studies, which were described in detail by Smith *et al.* (1995a). Here we provide an overview of the geospatial interface for KINEROS2, including data requirements and the major steps and methods used to derive model inputs. An example is provided illustrating how KINEROS2 can be used via AGWA for multi-scale watershed assessment. We conclude with a description of current and planned research and development that is designed to improve both KINEROS2 and AGWA and their usability for environmental management and planning.

5.1.1 KINEROS2

KINEROS2 is a distributed, physically based, event model describing the processes of interception, dynamic infiltration, surface runoff, and erosion from watersheds characterized by predominantly overland flow. The watershed is conceptualized as a cascade of planes and channels, over which flow is routed in a top-down approach using a finite difference solution of the one-dimensional kinematic wave equations. KINEROS2 may be used to evaluate the effects of various artificial features such as urban developments, detention reservoirs, circular conduits, or lined channels on flood hydrographs and sediment yield.

KINEROS2 originated at the US Department of Agriculture (USDA) Agricultural Research Service's (ARS) Southwest Watershed Research Center (SWRC) in the late 1960s as a model that routed runoff from hillslopes represented by a cascade of one-dimensional overland-flow planes contributing laterally to channels (Woolhiser, *et al.*, 1970). Rovey (1974) coupled interactive infiltration to this model and released it as KINGEN (Rovey

et al., 1977). After significant validation using experimental data, KINGEN was modified to include erosion and sediment transport as well as a number of additional enhancements, resulting in KINEROS (KINematic runoff and EROSion), which was released in 1990 (Woolhiser *et al.*, 1990) and described in some detail by Smith *et al.* (1995a). Subsequent research with, and application of, KINEROS has led to additional model enhancements and a more robust model structure, which have been incorporated into the latest version of the model: KINEROS2 (hereafter referred to as K2). K2 is open-source software that is distributed freely via the Internet, along with associated model documentation (www.tucson.ars.ag.gov/kineros).

5.1.2 AGWA

A geographic information system (GIS) user interface for K2, the Automated Geospatial Watershed Assessment (AGWA) tool, facilitates parameterization and calibration of the model. AGWA uses internationally available spatial datasets to delineate the watershed, subdivide it into model elements, and derive all necessary parameter inputs for each model element. AGWA also enables the spatial visualization and comparison of model results, and thus permits the assessment of hydrologic impacts associated with landscape change. The utilization of a GIS further provides a means of relating model results to other spatial information.

Spatially distributed data are required to develop inputs for K2, and the subdivision of watersheds into model elements and the assignment of appropriate parameters are both time-consuming and computationally complex. To apply K2 on an operational basis, there was thus a critical need for automated procedures that could take advantage of widely available spatial datasets and the computational power of geographic information systems (GIS). The AGWA GIS interface for K2 was developed in 2002 (Miller *et al.*, 2002) by the USDA-ARS, US Environmental Protection

Walnut Gulch Subwatershed No. 11 showing the watershed boundary and primary channel network (the pond catchment is a noncontributing area).

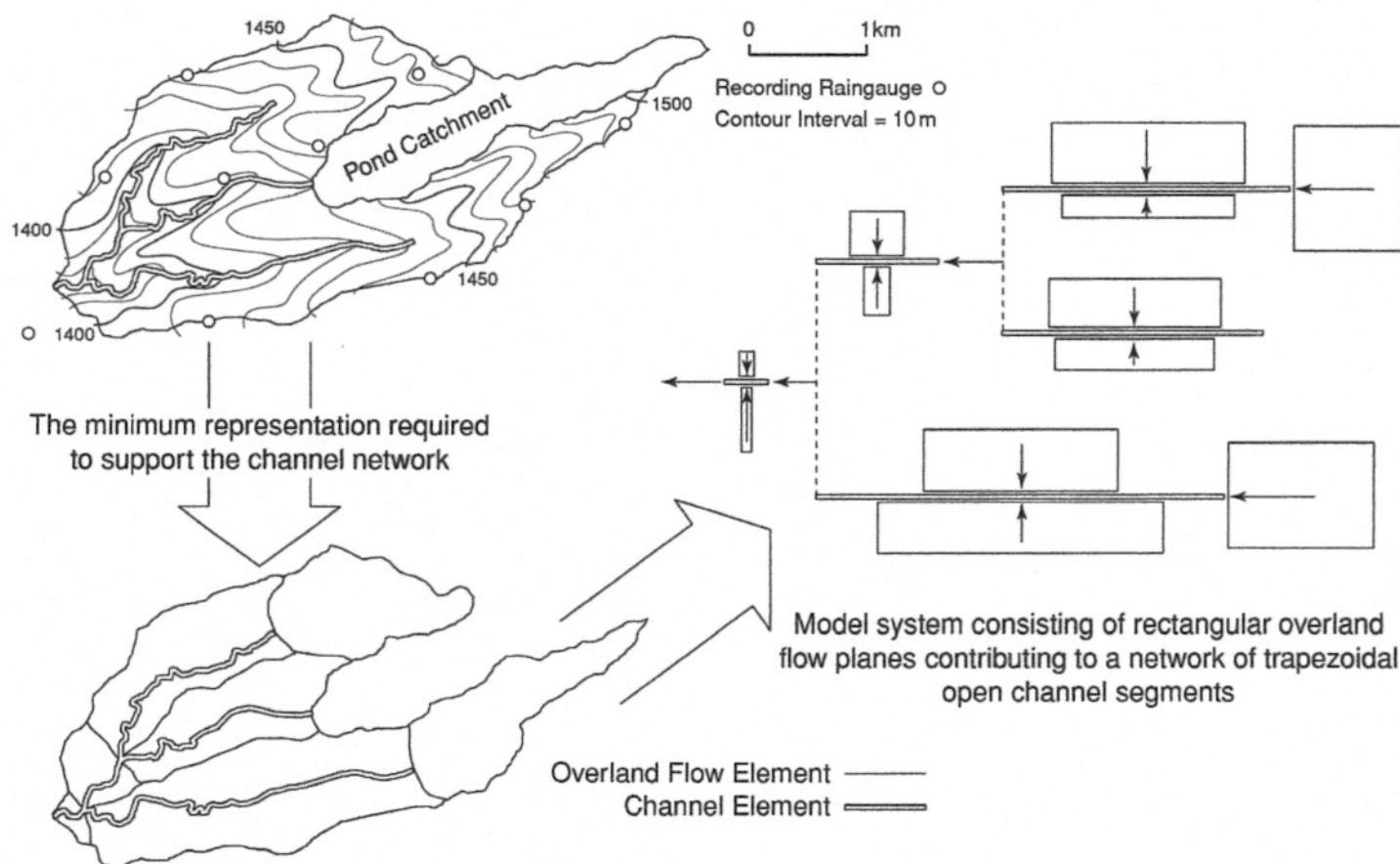


Figure 5.1 Illustration of how topographic data and channel network topology is abstracted into the simplified geometry defined by K2 model elements. Note that overland-flow planes are dimensioned to preserve average flow length, and therefore planes contributing laterally to channels generally do not have widths that match the channel length.

Agency (EPA) Office of Research and Development (ORD), and the University of Arizona (UA) to address this need.

AGWA is an extension for the Environmental Systems Research Institute's ArcView versions 3.X (ESRI, 2001), a widely used and relatively inexpensive PC-based GIS software package (trade names are mentioned solely for the purpose of providing specific information and do not imply recommendation or endorsement by the US EPA or USDA). The GIS framework of AGWA is ideally suited for watershed-based analysis in which landscape information is used for both deriving model input, and for visualization of the environment and modelling results. AGWA is distributed freely via the Internet as a modular, open-source suite of programs (www.tucson.ars.ag.gov/agwa or www.epa.gov/nerlesd1/land-sci/agwa).

5.2 KINEROS2 MODEL DESCRIPTION

5.2.1 Conceptual model elements

In K2, the watershed being modelled is conceptualized as a collection of spatially distributed model elements, of which there

can be several types. The model elements effectively abstract the watershed into a series of shapes, which can be oriented so that one-dimensional flow can be assumed. A typical subdivision, from topography to model elements, of a small watershed in the USDA-ARS Walnut Gulch Experimental is illustrated in Fig. 5.1. Further subdivision can be made to isolate hydrologically distinct portions of the watershed if desired (e.g., large impervious areas, abrupt changes in slope, soil type, or hydraulic roughness, etc.). As currently implemented, the computational order of the K2 model simulation must proceed from upslope/upstream elements to downstream elements. This is required to ensure that upper boundary conditions for the element being processed are always defined. Attributes for each of the model-element types are summarized in Table 5.1, and followed by more detailed descriptions in the text.

5.2.1.1 OVERLAND-FLOW ELEMENTS

Overland-flow elements are abstracted as regular, planar, rectangular surfaces with uniform parameter inputs. Non-uniform surfaces, such as converging or diverging contributing areas, or major breaks in slope, may be represented using a cascade of overland-flow elements, each with different parameter inputs.

Table 5.1 *KINEROS2 model-element types and attributes*

| Model element type | Attributes |
|----------------------|---|
| Overland flow | Planes; cascade allowed with varied lengths, widths, and slopes; microtopography |
| Urban overland | Mixed infiltrating/impervious with runoff-runon |
| Channels | Simple and compound trapezoidal |
| Detention Structures | Arbitrary shape, controlled outlet – discharge f (stage) |
| Culverts | Circular with free surface flow |
| Injection | Hydrographs and sedigraphs injected from outside the modelled system, or from a point discharge (e.g., pipe, drain) |

Microtopographic relief on upland surfaces can be represented by specifying the microtopographic relief height and mean spacing.

5.2.1.2 URBAN ELEMENTS

The urban element represents a composite of up to six overland-flow areas (Fig. 5.2), including various combinations of pervious and impervious surfaces contributing laterally to a paved, crowned street. This model element was originally conceived as a single residential or commercial lot; however, a contiguous series of similar lots along the same street can be combined into a single urban element. The aggregate model representation is offered instead of attempting to describe each roof, driveway, lawn, sidewalk, etc., as individual model elements. The urban element can receive upstream inflow (into the street), but not lateral inflow from adjacent urban or overland-flow elements. The relative proportions of the six overland-flow areas are specified as fractions of the total element area. It is not required to have all six types, but intervening connecting areas must be present if the corresponding indirectly connected area is specified. The element is modelled as rectangular.

5.2.1.3 CHANNEL ELEMENTS

Channels are defined by two trapezoidal cross-sections at the upstream and downstream ends of each reach. Geometric and

hydrologic parameters can be uniform, or vary linearly along a reach. If present, base flow can be represented with a constant inflow rate. Compound trapezoidal channels (Fig. 5.3) can be represented as a parallel pair of channels, each with its own hydraulic and infiltrative characteristics. For each channel, the geometric relations for cross-sectional area of flow A and wetted perimeter P are expressed in terms of the same depth, h , whose zero value corresponds to the level of the lowermost channel segment (Fig. 5.3). Note that the wetted perimeters do not include the interface where the two sections join, i.e., this constitutes a frictionless boundary (dotted vertical line). There is no need to explicitly account for mass transfer between the two channels, as it is implicit in the common depth (level water surface) requirement. However, for exchange of suspended sediment, a net transfer rate q_t is recovered via a mass balance after computation of h at the advanced time-step.

5.2.1.4 POND ELEMENTS

In addition to surface and channel elements, a watershed may contain detention storage elements, which receive inflow from up to ten upstream elements and two lateral elements and produce outflow from an uncontrolled outlet structure. This type of element can be used to represent a pond, or a flume or other flow-measuring structure with backwater storage. User-defined rating information is required to parameterize these elements. Infiltration, or seepage, is computed using a constant, user-defined saturated hydraulic conductivity.

5.2.1.5 CULVERT ELEMENTS

In an urban environment, circular conduits must be used to represent storm sewers. To apply the kinematic model, there must be no backwater, and the conduit is assumed to maintain free surface-flow conditions at all times – there can be no pressurization. A schematic drawing of a partially full circular section is shown in Fig. 5.4. There is assumed to be no lateral inflow. The upper boundary condition is a specified discharge as a function of time. No infiltration is computed for culvert elements.



Figure 5.2 Diagram illustrating the layout of an urban element and all six possible contributing areas.

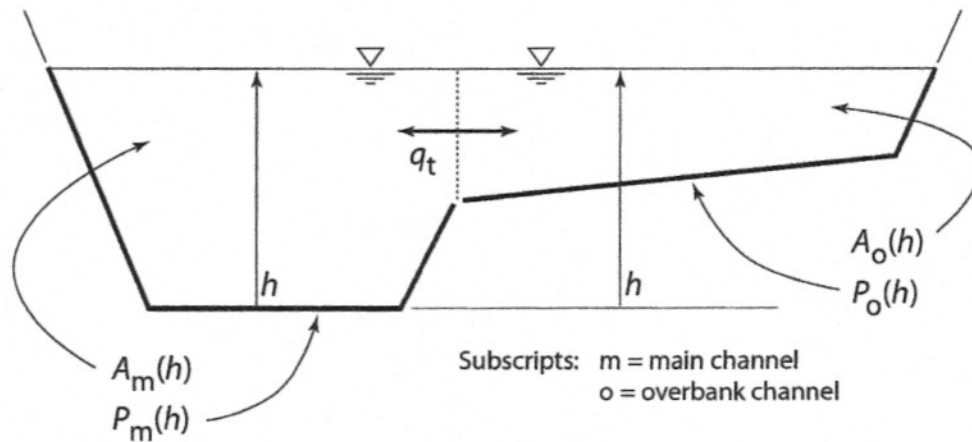


Figure 5.3 Diagram illustrating basic compound channel cross-section geometry

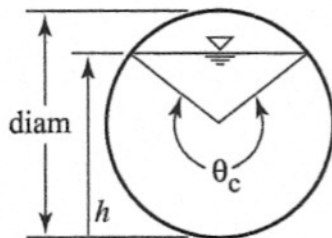


Figure 5.4 Diagram illustrating basic culvert geometry

5.2.1.6 INJECTION ELEMENTS

Injection elements provide a convenient means of introducing water and sediment from sources other than rainfall-derived runoff or base flows. Examples would include effluent from water treatment or industrial sources, or agricultural return flows. Data are provided as a text file listing time (min) and discharge (m^3/s) pairs plus up to five columns of corresponding sediment concentrations by particle class.

5.2.2 Mathematical and numerical model

5.2.2.1 RAINFALL

Rainfall data are entered as time-accumulated depth or time-intensity breakpoint pairs. A time–depth pair simply defines the total rainfall accumulated up to that time. A time–intensity pair defines the rainfall rate until the next data pair. If data are available as time–depth breakpoints, there is no advantage in converting them to intensity as the program must convert intensity to accumulated depth. Rainfall is modelled as spatially uniform over each element, but varies between elements if there is more than one rain gauge.

The spatial and temporal variability of rainfall is expressed by interpolation from rain gauge locations to each plane, pond or urban element (and optionally channels). An element's location is represented by a single pair of x, y coordinates, such as its aerial centroid. The interpolator attempts to find the three closest rain

gauges that enclose the element's coordinates. If such a configuration does not exist, it looks for the two closest gauges for which the element's coordinates lie within a strip bounded by two (parallel) lines that pass through the gauge locations and are perpendicular to the line connecting the two points. Finally, if two such points do not exist, the closest gauge alone is used.

If three points are used for the interpolation, the depth at any breakpoint time is represented by a plane passing through the depths above the three points for a given time-step, and the interpolated depth for the element is the depth above its coordinates (Fig. 5.5). For two points, a plane is defined by the two parallel lines, which are considered to be lines of constant depth.

Once the configuration is determined and the spatial interpolating coefficients are computed, an extended set of breakpoint times is constructed as the union of all breakpoint times from the two or three gauges. Final breakpoint depths are computed using the extended set of breakpoint times, interpolating depths within each set of gauge data when necessary. If initial soil saturation is specified in the rainfall file, it will be interpolated using the same spatial interpolation coefficients.

5.2.2.2 INTERCEPTION

As implemented in K2, interception is the portion of rainfall that initially collects and is retained on vegetative surfaces. The effect of interception is controlled by two parameters: the interception depth and the fraction of the surface covered by intercepting vegetation. The interception-depth parameter reflects the average depth of rainfall retained by the particular vegetation type or mixture of vegetation types present on the surface. Rainfall rate is reduced by the cover fraction (i.e., a cover fraction equal to 0.50 gives a 50% reduction) until the amount retained reaches the interception depth.

5.2.2.3 INFILTRATION

The conceptual model of soil hydrology in K2 represents a soil of either one or two layers, with the upper layer of arbitrary depth,

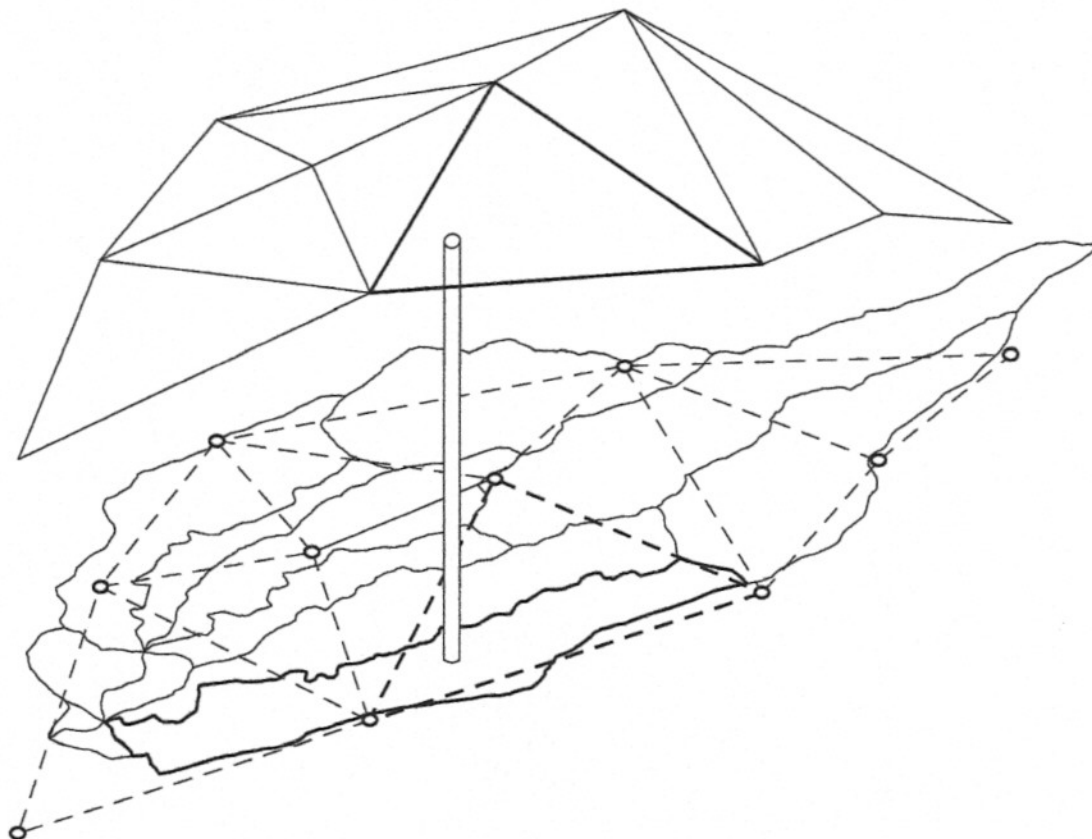


Figure 5.5 Diagrammatic representation of the K2 rainfall interpolation procedure

exhibiting log-normally distributed values of saturated hydraulic conductivity, K_S . The surface of the soil exhibits microtopographic variations that are characterized by a mean micro-rill spacing and height. This latter feature is significant in the model, since one of the important aspects of the K2 hydrology is an explicit interaction of surface flow and infiltration. Infiltration may occur from either rainfall directly on the soil or from ponded surface water created from previous rainfall excess. Also involved in this interaction, as discussed below, is the small-scale random variation of K_S . All of the facets of K2 infiltration theory are presented in much greater detail in Smith *et al.* (2002).

Basic infiltrability

Infiltrability, f_c , is the rate at which soil will absorb water (vertically) when there is an unlimited supply at the surface. Infiltration rate, f , is equal to rainfall, $r(t)$, until this limit is reached. K2 uses the Parlange 3-Parameter model for this process (Parlange *et al.*, 1982), in which the models of Green and Ampt (1911) and Smith and Parlange (1978) are included as the two limiting cases. A scaling parameter, γ , is the third parameter in addition to the two basic parameters K_S and capillary length scale, G . Most soils exhibit infiltrability behavior intermediate to these two models, and K2 uses a weighting “ γ ” value of 0.85. The state variable for infiltrability is the initial water content, in the form of the soil saturation deficit, $G\Delta\theta_i$, defined as the saturated water content minus the initial water content. In terms of these variables, the

basic model is:

$$f_c = K_S \left[1 + \frac{\gamma}{\exp\left(\frac{\gamma I}{G\Delta\theta_i}\right) - 1} \right]. \quad (5.1)$$

The K2 infiltration model employs the *infiltrability depth approximation* (IDA) from Smith *et al.* (2002) in which f_c is described as a function of infiltrated depth I . This approach derives from the “time compression” approximation earlier suggested by Reeves and Miller (1975): time is not compressed, but I is a surrogate for time as an independent variable. This form of infiltrability model eliminates the separate description of ponding time and the decay of f after ponding.

Small-scale spatial variability

The infiltrability model of K2 incorporates the coefficient of variation of K_S , CV_K , as described by Smith and Goodrich (2000). Assuming that K_S is distributed log-normally, there will for all normal values of rain intensity r be some portion of the surface for which $r < K_S$. Thus for that area there will be no potential runoff. Smith and Goodrich (2000) simulated ensembles of distributed point infiltration and arrived at a function for infiltrability

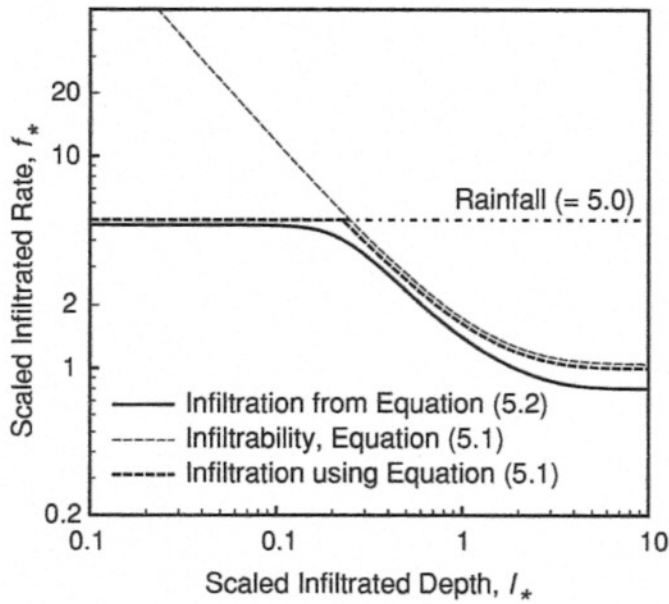


Figure 5.6 Graph showing a comparison of the infiltrability function with and without consideration of randomly varying K_S

which closely describes this ensemble infiltration behavior:

$$f_{e^*} = 1 + (r_{e^*} - 1) \left\{ 1 + \left[\frac{(r_{e^*} - 1)}{\gamma} (e^{\gamma l_{e^*}} - 1) \right]^c \right\}_{r_{e^*} > 1}^{-1/c}, \quad (5.2)$$

in which f_{e^*} and r_{e^*} are infiltrability and rain rate scaled on the ensemble effective asymptotic K_S value. This effective ensemble K_e is the appropriate K_S parameter to use in the infiltrability function for an ensemble, and is a function of CV_K and r_{e^*} ; the ratio of r to ensemble mean of K_S defined as $\xi(K)$. Smith and Goodrich (2000) describe how effective K_e drops significantly below $\xi(K)$ for low relative rain rates and high relative values of CV_K .

Equation (5.2) also scales l by the parameter pair $G\Delta\theta_i$. The additional parameter c is a function only of CV_K and the value of r . There is evidence in watershed runoff measurements (Smith and Goodrich, 2000) that this function is more appropriate for watershed areas than the basic (uniform K_S) relation of Equation (5.1). Figure 5.6 compares Equation (5.2) for $CV_K = 0.8$ to Equation (5.1), in which CV_K is implicitly zero. Note that Equation (5.2) does not have a ponding point, but rather exhibits a gradual evolution of runoff, and thus Equation (5.2) describes infiltration rate rather than infiltrability.

Infiltration with two-layer soil profiles

For a soil with two layers, either layer can be flow limiting and thus can be the infiltration control layer, depending on the soil properties, thickness of the surface layer, and the rainfall rate. There are several possibilities, most of which have been discussed by Corradini *et al.* (2000) and Smith *et al.* (1993). K2 attempts to model all cases in a realistic manner, including the redistribution

of soil water during periods when r is less than K_S and thus runoff is not generated from rainfall.

Upper soil control: For surface soil layers that are sufficiently deep, this case [$r > K_{S1}$] resembles a single soil profile. However, when the wetting front reaches the layer interface, the capillary drive parameter and the effective value of K_S for Equation (5.1) must be modified. The effective parameters for this case were discussed by Smith (1990). The effective K_S parameter, K_4 , is found by solving the steady unsaturated flow equation with matching values of soil capillary potential at the interface.

Lower soil control: When the condition $K_{S1} > r > K_{S2}$ occurs, the common runoff mechanism called saturation runoff may occur. K2 treats the limitation of flow through the lower soil by application of Equation (5.1) or (5.2) to flow through the layer interface, and when that water which cannot enter the lower layer has filled the available pore space in the upper soil, runoff is considered to begin. The available pore space in the upper soil is the initial deficit $\Delta\theta_{1i}$ less rainwater in transit through the upper soil layer. For reasonably deep surface-soil layers, it is possible for control to shift from the lower to the upper if the rainfall rate increases to sufficiently exceed K_{S1} before the surface layer is filled from flow limitations into the lower layer.

An example of runoff generation from single and two-layer soil profiles is illustrated in Fig. 5.7. Note that in both profiles the top soils have identical porosity and saturated hydraulic conductivity. The shallow top layer in the two-layer case has significantly less available pore space to store and transmit infiltrated water to the lower, less permeable, soil layer. The burst of rainfall occurring at roughly 850 minutes into the event produces identical Hortonian runoff from both profiles for approximately 40 minutes. The upper soil layer is controlling in both profiles and runoff is produced by infiltration excess. The long, low-intensity period of rainfall between 950 and 1850 minutes is fully absorbed by both soil profiles, but is effectively filling the available pore space in the shallow upper layer of the two-layer profile. When the rainfall intensity increases at approximately 1850 minutes to around 5 mm/hr ($r < K_S$ of the upper soil layer), runoff is generated from the shallow profile as the lower soil layer in the two-layer systems is now controlling and runoff generation occurs via saturation excess. The single layer profile again generates runoff via infiltration excess when the rainfall intensity increases (at ~2010 minutes) above the infiltrability of the soil.

Redistribution and initial wetting

Rainfall patterns of all types and rainfall rates of any value should be accommodated realistically in a robust infiltration model. This includes the effect on runoff potential of an initial storm period of very low rainfall rates, and the reaction of the soil infiltrability to periods within the storm of low or zero rainfall rates. K2 simulates the wetting-zone changes due to these conditions with

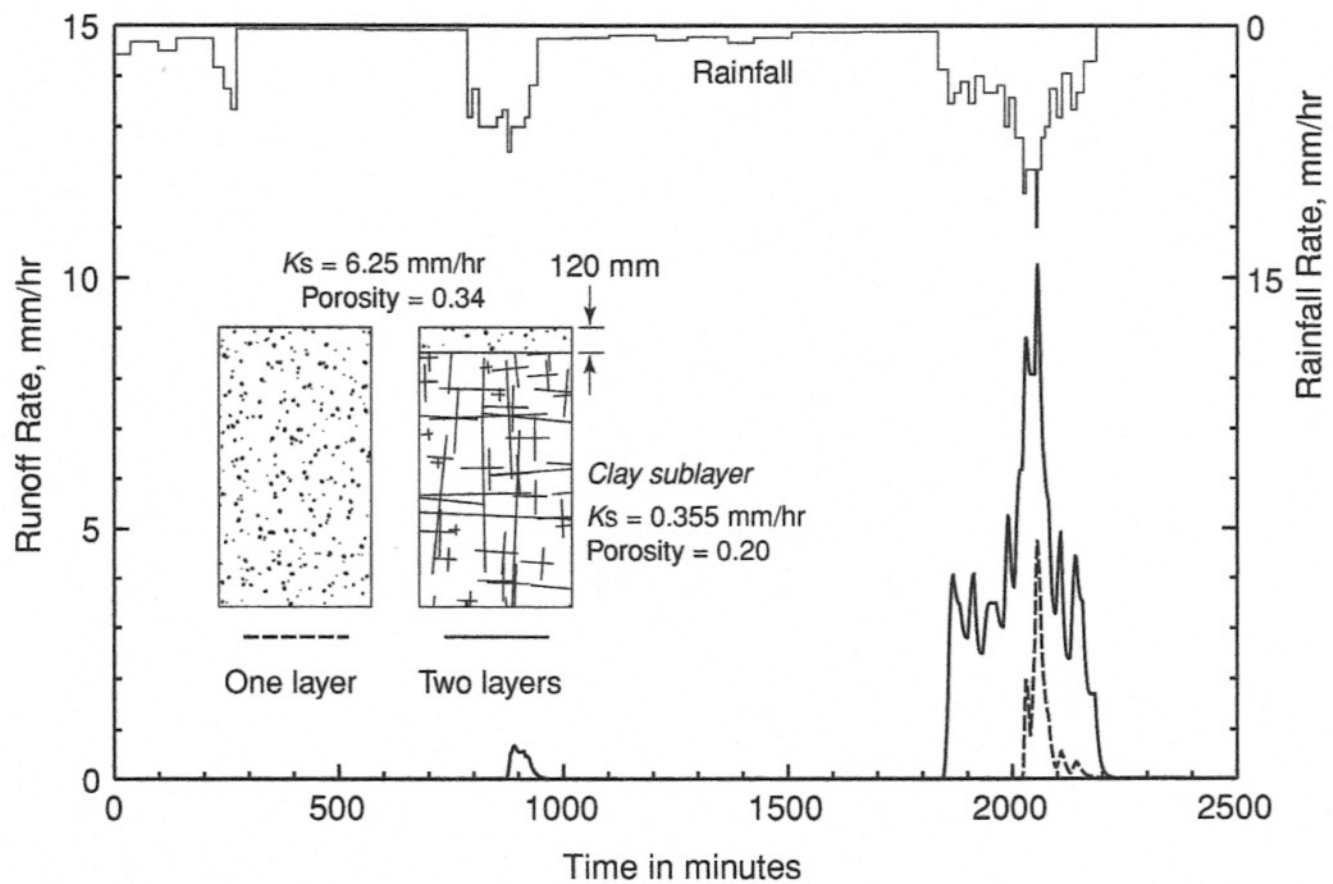


Figure 5.7 Graph of computed runoff rate for simulations based on one- and two-layer soil profiles illustrating infiltration- and saturation-excess runoff generation

an approximation described by Smith *et al.* (1993) and Corradini *et al.* (2000). Briefly, the wetting profile of the soil is described by a water-balance equation in which the additions from rainfall are balanced by the increase in the wetted zone value of two and the extension of the wetted zone depth due to the capillary drive of the wetting front. The soil wetted shape is treated as a similar shape of depth Z with volume $\Xi Z(\Delta\theta_0 - \Delta\theta_1)$, where Ξ is a constant scale factor defined in Smith *et al.* (1993). Space does not permit detailed description here, but the method is applicable to prewetting of the soil as well as the decrease in $\Delta\theta_0$ during a storm hiatus. It is also applicable, with modification, to soils with two layers.

5.2.2.4 OVERLAND FLOW

The appearance of free water on the soil surface, called ponding, gives rise to runoff in the direction of the local slope (Fig. 5.8). Rainfall can produce ponding by two mechanisms, as outlined in the infiltration section. The first mechanism involves a rate of rainfall, which exceeds the infiltrability of the soil at the surface. The second mechanism is soil filling, when a soil layer deeper in the soil restricts downward flow and the surface layer fills its available porosity. In the first mechanism, the surface-soil water-pressure head is not more than the depth of water, and decreases

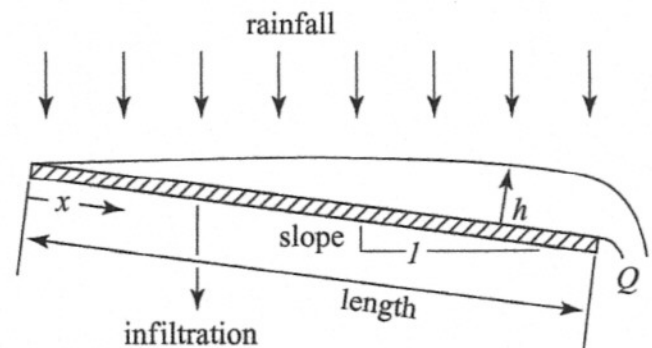


Figure 5.8 Definition sketch for overland flow

with depth, while in the second mechanism, soil water-pressure head increases with depth until the restrictive layer is reached.

Viewed at a very small scale, overland flow is an extremely complex three-dimensional process. At a larger scale, however, it can be viewed as a one-dimensional flow process in which flux is related to the unit area storage by a simple power relation:

$$Q = \alpha h^m, \quad (5.3)$$

where Q is discharge per unit width and h is the storage of water per unit area. Parameters α and m are related to slope, surface roughness, and flow regime. Equation (5.3) is used in conjunction

with the equation of continuity:

$$\frac{\partial h}{\partial t} + \frac{\partial Q}{\partial x} = q(x, t), \quad (5.4)$$

where t is time, x is the distance along the slope direction, and q is the lateral inflow rate. For overland flow, Equation (5.3) may be substituted into Equation (5.4) to obtain:

$$\frac{\partial h}{\partial t} + \alpha m h^{m-1} \frac{\partial h}{\partial x} = q(x, t). \quad (5.5)$$

By taking a larger-scale, one-dimensional approach it is assumed that Equation (5.5) describes normal flow processes; it is not assumed that overland-flow elements are flat planes characterized by uniform depth sheet flow.

The kinematic-wave equations are simplifications of the de Saint Venant equations, and do not preserve all of the properties of the more complex equations, such as backwater and diffusive-wave attenuation. Attenuation does occur in kinematic routing from shocks or from spatially variable infiltration. The kinematic routing method, however, is an excellent approximation for most overland-flow conditions (Woolhiser and Liggett, 1967; Morris and Woolhiser, 1980).

Boundary conditions

The depth or unit storage at the upstream boundary must be specified to solve Equation (5.5). If the upstream boundary is a flow divide, the boundary condition is

$$h(0, t) = 0. \quad (5.6)$$

If another surface is contributing flow at the upper boundary, the boundary condition is

$$h(0, t) = \left[\frac{\alpha_u h_u(L, t)^{m_u} W_u}{\alpha W} \right]^{\frac{1}{m}}, \quad (5.7)$$

where subscript u refers to the upstream surface, W is width and L is the length of the upstream element. This merely states an equivalence of discharge between the upstream and downstream elements.

Recession and microtopography

Microtopographic relief can play an important role in determining hydrograph shape (Woolhiser *et al.*, 1997). The effect is most pronounced during recession, when the extent of soil covered by the flowing water determines the opportunity for water loss by infiltration. K2 provides for treatment of this relief by assuming the relief geometry has a maximum elevation, and that the area covered by surface water varies linearly with elevation up to this maximum (Fig. 5.9). The geometry of microtopography is completed by specifying a relief scale, which geometrically represents the mean spacing between relief elements.

Given the conceptual relation presented in Figure 5.9, the effective mean hydraulic depth, h_m , is computed as the cross-sectional

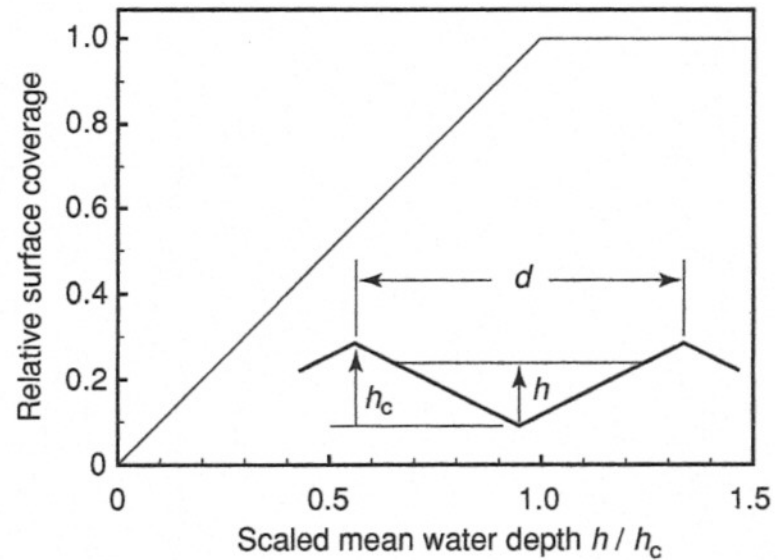


Figure 5.9 Graph showing the assumed relation of covered surface area to scaled mean water depth. Parameter h_c is the microtopographic relief height and d is the mean microtopographic spacing.

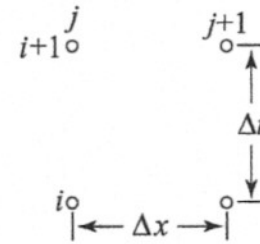


Figure 5.10 Notation for space and time dimensions of the finite difference grid

area of flow divided by the width of the element. The relation here is scaled, and the maximum topographic relief, h_c , is a parameter that can be user-defined. Infiltration from the portion of the surface covered by water proceeds at the infiltrability rate, and the remaining area will have a value of f determined by the rainfall rate. Thus infiltration proceeds during receding flows depending on the microtopography.

Numerical solution

KINEROS2 solves the kinematic-wave equations using a four-point implicit finite difference method. The finite difference form for Equation (5.5) is

$$\begin{aligned} & h_{j+1}^{i+1} - h_{j+1}^i + h_j^{i+1} - h_j^i + \frac{2\Delta t}{\Delta x} \left\{ \theta_w \left[\alpha_{j+1}^{i+1} (h_{j+1}^{i+1})^m \right. \right. \\ & \left. \left. - \alpha_j^{i+1} (h_j^{i+1})^m \right] + (1 - \theta_w) \left[\alpha_{j+1}^i (h_{j+1}^i)^m - \alpha_j^i (h_j^i)^m \right] \right\} \\ & - \Delta t (\bar{q}_{j+1} + \bar{q}_j) = 0, \end{aligned} \quad (5.8)$$

where θ_w is a weighting parameter (usually 0.6 to 0.8) for the x derivatives at the advanced time-step. The notation for this method is shown in Fig. 5.10.

A solution is obtained by Newton's method (sometimes referred to as the Newton–Raphson technique). While the solution is unconditionally stable in a linear sense, the accuracy is highly dependent on the size of Δx and Δt values used. The difference scheme is nominally of first-order accuracy.

Roughness relationships

Two options for α and m in Equation (5.5) are provided in K2:

- (1) The Manning hydraulic resistance law may be used. In this option

$$\alpha = 1.49 \frac{S^{1/2}}{n} \quad \text{and} \quad m = \frac{5}{3}, \quad (5.9)$$

where S is the slope, n is a Manning's roughness coefficient for overland flow, and English units are used.

- (2) The Chezy law may be used. In this option,

$$\alpha = CS^{1/2} \quad \text{and} \quad m = \frac{3}{2}, \quad (5.10)$$

where C is the Chezy friction coefficient.

5.2.2.5 CHANNEL FLOW

Unsteady, free-surface flow in channels is also represented by the kinematic approximation to the unsteady, gradually varied flow equations. Channel segments may receive uniformly distributed but time-varying lateral inflow from overland-flow elements on either or both sides of the channel, from one or two channels at the upstream boundary, and/or from an upland area at the upstream boundary. The dimensions of overland-flow elements are chosen to completely cover the watershed, so rainfall on the channel is not considered directly.

The continuity equation for a channel with lateral inflow is:

$$\frac{\partial A}{\partial t} + \frac{\partial Q}{\partial x} = q_c(x, t), \quad (5.11)$$

where A is the cross-sectional area, Q is the channel discharge, and $q_c(x, t)$ is the net lateral inflow per unit length of channel. Under the kinematic assumption, Q can be expressed as a unique function of A , and Equation (5.11) can be rewritten as:

$$\frac{\partial A}{\partial t} + \frac{\partial Q}{\partial A} \frac{\partial A}{\partial x} = q_c(x, t). \quad (5.12)$$

The kinematic assumption is embodied in the relationship between channel discharge and cross-sectional area such that:

$$Q = \alpha R^{m-1} A, \quad (5.13)$$

where R is the hydraulic radius. If the Chezy relationship is used, $\alpha = CS^{1/2}$ and $m = 3/2$. If the Manning equation is used, $\alpha = 1.49S^{1/2}/n$ and $m = 5/3$. Channel cross-sections may be approximated as trapezoidal or circular, as shown in Figs. 5.3 and 5.4.

Compound channels

K2 contains the ability to route flow through channels with a significant overbank region. The channel may in this case be composed of a smaller channel incised within a larger flood plane or swale. The compound channel algorithm is based on two independent kinematic equations (one for the main channel and one for the overbank section), which are written in terms of the same datum for flow depth. In writing the separate equations, it is explicitly assumed that no energy transfer occurs between the two sections, and upon adding the two equations the common datum implicitly requires the water-surface elevation to be equal in both sections (Fig. 5.3). However, flow may move from one part of the compound section to another. Such transfer will take with it whatever the sediment concentration may be in that flow when sediment routing is simulated. Each section has its own set of parameters describing the hydraulic roughness, bed slope, and infiltration characteristics. A compound-channel element can be linked with other compound channels or with simple trapezoidal channel elements. At such transitions, as at other element boundaries, discharge is conserved and new heads are computed downstream of the transition.

Base flow

K2 allows the user to specify a constant base flow in a channel, which is added at a fractional rate at each computational node along the channel to produce the designated flow at the downstream end of the reach. This feature allows simulation of floods that occur in excess of an existing base discharge, but requires foreknowledge of where those flows originate and at what rate.

Channel infiltration

In arid and semi-arid regions, infiltration into channel alluvium may significantly affect runoff volume and peak discharge. If the channel infiltration option is selected, Equation (5.2) is used to calculate accumulated infiltration at each computational node, beginning either when lateral inflow begins or when an advancing front has reached that computational node. Because the trapezoidal channel simplification introduces significant error in the area of channel covered by water at low flow rates (Unkrich and Osborn, 1987), an empirical expression is used to estimate an "effective wetted perimeter." The equation used in K2 is:

$$p_e = \min \left[\frac{h}{0.15\sqrt{BW}}, 1 \right] p, \quad (5.14)$$

where p_e is the effective wetted perimeter for infiltration, h is the depth, BW is the bottom width, and p is the channel wetted perimeter at depth h . This equation states that p_e is smaller than p until a threshold depth is reached, and at depths greater than the threshold depth, p_e and p are identical. The channel loss rate is obtained by multiplying the infiltration rate by the effective

wetted perimeter. A two-layer soil representation is also allowed in channels.

Culverts

The most general discharge relationship and the one often used for flow in pipes is the Darcy–Weisbach formula:

$$S_f = \frac{f_D}{4R} \frac{u^2}{2g}, \quad (5.15)$$

where S_f is the friction slope, f_D is the Darcy–Weisbach friction factor, and u is the velocity (Q/A). Under the kinematic assumption, the conduit slope S may be substituted for S_f in Equation (5.15), so that

$$u = 2\sqrt{\frac{2g}{f_D}RS}. \quad (5.16)$$

Discharge is computed by using Equation (5.16), and a specialized relationship between channel discharge and cross-sectional area:

$$Q = \frac{\alpha A^m}{p^{m-1}} \quad (5.17)$$

where p is the wetted perimeter, α is $[8gS/f_D]^{1/2}$, and $m = 3/2$. Geometric relationships for partially full conduits are discussed further in the original KINEROS documentation (Woolhiser *et al.*, 1990).

Numerical method for channels

The kinematic equations for channels are solved by a four-point implicit technique similar to that for overland-flow surfaces, except that A is used instead of h , and the geometric changes with depth are considered.

5.2.2.6 POND FLOW

In-channel detention structures are modelled as simple reservoirs. Outflow is assumed to be solely a function of water depth, so the dynamics of the storage are described by the mass-balance and outflow equations:

$$\frac{dV}{dt} = q_I - q_O - A_p f_c, \quad (5.18)$$

in which

- V = storage volume [L^3],
- q_I = inflow rate [L^3/T],
- q_O = outflow rate [L^3/T],
- A_p = pond surface area [L^2]
- f_c = pond infiltration loss rate [L/T].

Reservoir geometry is described by a user-defined rating table for V , A_p , and q_O . Equation (5.18) is written in finite difference form over a time interval t and the stage at time $t + \Delta t$ is determined using a hybrid Newton–Raphson/bisection method. For a given V , A_p and q_O are estimated using log–log interpolation.

5.2.2.7 EROSION AND SEDIMENTATION

As an optional feature, K2 can simulate the movement of eroded soil in addition to the movement of surface water. K2 accounts separately for erosion caused by raindrop energy (splash erosion) and erosion caused by flowing water (hydraulic erosion). Erosion is computed for upland, channel, and pond elements.

The general equation used to describe the sediment dynamics at any point along a surface flow path is a mass-balance equation similar to that for kinematic water flow (Bennett, 1974):

$$\frac{\partial(AC_s)}{\partial t} + \frac{\partial(QC_s)}{\partial x} - e(x, t) = q_s(x, t), \quad (5.19)$$

in which

- C_s = sediment concentration [L^3/L^3],
- Q = water discharge rate [L^3/T],
- A = cross-sectional area of flow [L^2],
- e = rate of erosion of the soil bed [L^2/T],
- q_s = rate of lateral sediment inflow for channels [$L^3/T/L$].

For upland surfaces, it is assumed that e is composed of two major components – production of eroded soil by splash of rainfall on bare soil, and hydraulic erosion (or deposition) due to the interplay between the shearing force of water on the loose soil bed and the tendency of soil particles to settle under the force of gravity. Thus e may be positive (increasing concentration in the water) or negative (deposition). Net erosion is a sum of splash erosion rate as e_s and hydraulic erosion rate as e_h :

$$e = e_s + e_h. \quad (5.20)$$

Splash erosion

Based on limited experimental evidence, the splash erosion rate can be approximated as a function of the square of the rainfall rate (Meyer and Wischmeier, 1969). This relationship is used in K2 to estimate the splash erosion rate as follows:

$$\begin{aligned} e_s &= c_f k(h) r^2, & q > 0 \\ e_s &= 0, & q < 0, \end{aligned} \quad (5.21)$$

in which c_f is a constant related to soil and surface properties, and $k(h)$ is a reduction factor representing the reduction in splash erosion caused by increasing depth of water. The function $k(h)$ is 1.0 prior to runoff and its minimum is zero for very deep flow; it is given by the empirical expression:

$$k(h) = \exp(-c_h h) \quad (5.22)$$

The parameter c_h represents the damping effectiveness of surface water, and does not vary widely. Both c_f and $k(h)$ are always positive, so e_s is always positive when there is rainfall and a positive rainfall excess (q).

Hydraulic erosion

The hydraulic erosion rate e_h represents the rate of exchange of sediment between the flowing water and the soil over which it flows, and may be either positive or negative. K2 assumes that for any given surface-water flow condition (velocity, depth, slope, etc.), there is an equilibrium concentration of sediment that can be carried if that flow continues steadily. The hydraulic erosion rate (e_h) is estimated as being linearly dependent on the difference between the equilibrium concentration and the current sediment concentration. In other words, hydraulic erosion/deposition is modelled as a kinetic transfer process:

$$e_h = c_g(C_m - C_s)A, \quad (5.23)$$

in which C_m is the concentration at equilibrium transport capacity, $C_s = C_s(x, t)$ is the current local sediment concentration, and c_g is a transfer-rate coefficient [T^{-1}]. Clearly, the transport capacity is important in determining hydraulic erosion, as is the selection of transfer-rate coefficient. Conceptually, when deposition is occurring, c_g is theoretically equal to the particle-settling velocity divided by the hydraulic depth, h . For erosion conditions on cohesive soils, the value of c_g must be reduced, and v_s/h is used as an upper limit for c_g .

Microtopography

The treatment of infiltration and microtopography also interacts with erosion as the effective mean hydraulic depth and related velocity drive the hydraulic portion of erosion. In addition it affects the percentage of the surface that is subject to splash erosion from raindrop impact. This conceptualization of microtopography does not directly define a rill-inter-rill region in terms of erosion treatment. Both "rill" and "interrill" processes can occur simultaneously in shallow flow as splash erosion can occur on the sides of rills and in rills when flow is sufficiently shallow so that raindrop momentum is transmitted to the soil surface (Smith *et al.*, 1995b).

Transport capacity

Transport capacity is determined using the relation of Engelund and Hansen (1967):

$$C_m = \frac{0.05uu_*^3}{g^2dh(\gamma_s - 1)^2}, \quad (5.24)$$

in which

- u is velocity [L/T],
- u_* is shear velocity, defined as \sqrt{ghS} ,
- d is particle diameter [L],
- γ_s is suspended specific gravity of the particles, $\gamma_s - 1$,
- h is water depth [L].

Particle settling velocity

Settling velocity is calculated from particle size and density assuming the particles have drag characteristics and terminal-fall velocities similar to those of spheres (Fair and Geyer, 1954). This relation is:

$$v_s^2 = \frac{4g(\rho_s - 1)}{3C_D} \quad (5.25)$$

in which C_D is the particle drag coefficient. The drag coefficient is a function of particle Reynolds number:

$$C_D = \frac{24}{R_n} + \frac{3}{\sqrt{R_n}} + 0.34, \quad (5.26)$$

in which R_n is the particle Reynolds number, defined as:

$$R_n = \frac{v_s d}{\nu}, \quad (5.27)$$

where ν is the kinematic viscosity of water [L^2/T]. Settling velocity of a particle is found by solving Equations (5.25), (5.26), and (5.27) for v_s .

Treating a range of particle sizes

Erosion relations are applied to each of up to five particle-size classes, which are used to describe the range of particle sizes found in typical soils. Our experimental and theoretical understanding of the dynamics of erosion for a mix of particle sizes is incomplete. It is not clear, for example, exactly what results when the distribution of relative particle sizes is contradictory to the distribution of their relative transport capacities. In larger particles on stream bottoms, armoring will ultimately occur when smaller, more transportable particles are selectively removed, leaving behind an "armor" of large particles. For the smaller particle sizes found in the shallower flows and rapidly changing flow conditions characteristic of overland flow, however, there is considerably less understanding of the relations. Sufficient knowledge does exist, however, to use the following assumptions in the formulation of K2:

- (1) If the largest particle size in a soil of mixed sizes is below its erosion threshold, the erosion of smaller sizes will be limited, since otherwise armoring will soon stop the erosion process.
- (2) When erosive conditions exist for all particle sizes, particle erosion rates will be proportional to the relative occurrence of the particle sizes in the surface soil. The same is true of erosion by rain splash.
- (3) Particle settling velocities, when concentrations exceed transportability, are independent of the concentration of other particle sizes.

Treatment of a mix of sizes is most critical for cases where the sediment characterizing the bed of the channels is significantly different from that of the upland slopes, and where impoundments exist in which there is significant opportunity for selective settling.

Numerical method for sediment transport

Equations (5.19)–(5.24) are solved numerically at each time-step used by the surface-water flow equations, and for each particle-size class. A four-point finite-difference scheme is again used; but iteration is not required since, given current and immediate past values for A and Q and previous values for C_s , the finite difference form of this equation is explicit, i.e.:

$$C_{s,j+1}^{i+1} = f(C_{s,j}^i, C_{s,j+1}^i, C_{s,j}^{i+1}). \quad (5.28)$$

The value of C_m is found from Equation (5.24) using current hydraulic conditions.

Initial conditions for erosion

When runoff commences during a period when rainfall is creating splash erosion, the initial condition on the vector C_s should not be taken as zero. The initial sediment concentration at ponding, $C_s(t = t_p)$, can be found by simplifying Equation (5.19) for conditions at that time. Variation with respect to x vanishes, and hydraulic erosion is zero. Then:

$$\frac{\partial(AC_s)}{\partial t} = e(x, t) = c_f r q - C_s v_s, \quad (5.29)$$

where $k(h)$ is assumed to be 1.0 since depth is zero. Since A is zero at time of ponding, and dA/dt is the rainfall excess rate (q), expanding the left-hand side of Equation (5.29) results in:

$$C_s(t = t_p) = \frac{c_f r q}{q + v_s}. \quad (5.30)$$

The sediment concentration at the upper boundary of a single overland flow element, $C_s(0, t)$, is given by an expression identical to Equation (5.30), and a similar expression is used at the upper boundary of a channel.

Channel erosion and sediment transport

The general approach to sediment-transport simulation for channels is nearly the same as that for upland areas. The major difference in the equations is that splash erosion (e_s) is neglected in channel flow, and the term q_s becomes important in representing lateral inflows. Equations (5.19) and (5.23) are equally applicable to either channel or distributed surface flow, but the choice of transport-capacity relation may be different for the two flow conditions. For upland areas, q_s will be zero, whereas for channels it will be the important addition that comes with lateral inflow from surface elements. The close similarity of the treatment of the two types of elements allows the program to use the same algorithms for both types of elements.

The erosion computational scheme for any element uses the same time and space steps employed by the numerical solution of the surface-water flow equations. In that context, Equations (5.19) and (5.23) are solved for $C_s(x, t)$, starting at the first node

below the upstream boundary, and from the upstream conditions for channel elements. If there is no inflow at the upper end of the channel, the transport capacity at the upper node is zero and any lateral input of sediment will be subject there to deposition. The upper boundary condition is then:

$$C_s(0, t) = \frac{q_s}{q_c + v_s W_B}, \quad (5.31)$$

where W_B is the channel bottom width. $A(x, t)$ and $Q(x, t)$ are assumed to be known from the surface-water solution.

5.3 AGWA GIS INTERFACE

5.3.1 Background

AGWA was developed as a collaborative effort between the USDA-ARS, EPA-ORD, and UA under the following guidelines: (1) that its parameterization routines be simple, direct, transparent, and repeatable; (2) that it be compatible with commonly available GIS data layers; and (3) that it be useful for scenario development and assessment at multiple scales.

Over the past decade numerous significant advances have been made in the linkage of GIS and various research and application models (e.g., HEC-GeoHMS, USACE, 2003; AGNPS, Bingner and Theurer, 2001; BASINS, Lahlou *et al.*, 1998). These GIS-based systems have greatly enhanced the capacity for research scientists to develop and apply models due to the improved data management and rapid parameter-estimation tools that can be built into a GIS driver. As one of these GIS-based modelling tools, AGWA provides the functionality to conduct all phases of a watershed assessment for two widely used watershed hydrologic models: K2 and the Soil and Water Assessment Tool (SWAT; Arnold *et al.*, 1995). SWAT is a continuous-simulation model for use in large (river-basin scale) watersheds and in humid regions, where K2 cannot be applied with confidence. The AGWA tool provides an intuitive interface to these models for performing multi-scale modelling and change assessment in a variety of geographies. Data requirements include elevation, classified land cover, soils, and precipitation data, all of which are typically available at no cost over the Internet. Model input parameters are derived directly from these data using optimized look-up tables that are provided with the tool.

AGWA shares the same ArcView GIS framework as the US EPA Analytical Tools Interface for Landscape Assessment (ATtILA; Ebert and Wade, 2004), and Better Assessment Science Integrating Point and Nonpoint Sources (BASINS; Lahlou *et al.*, 1998), and can be used in concert with these tools to improve scientific understanding (Miller *et al.*, 2002). Watershed analyses may benefit from the integration of multiple model outputs as this approach facilitates comparative analyses and is particularly valuable for

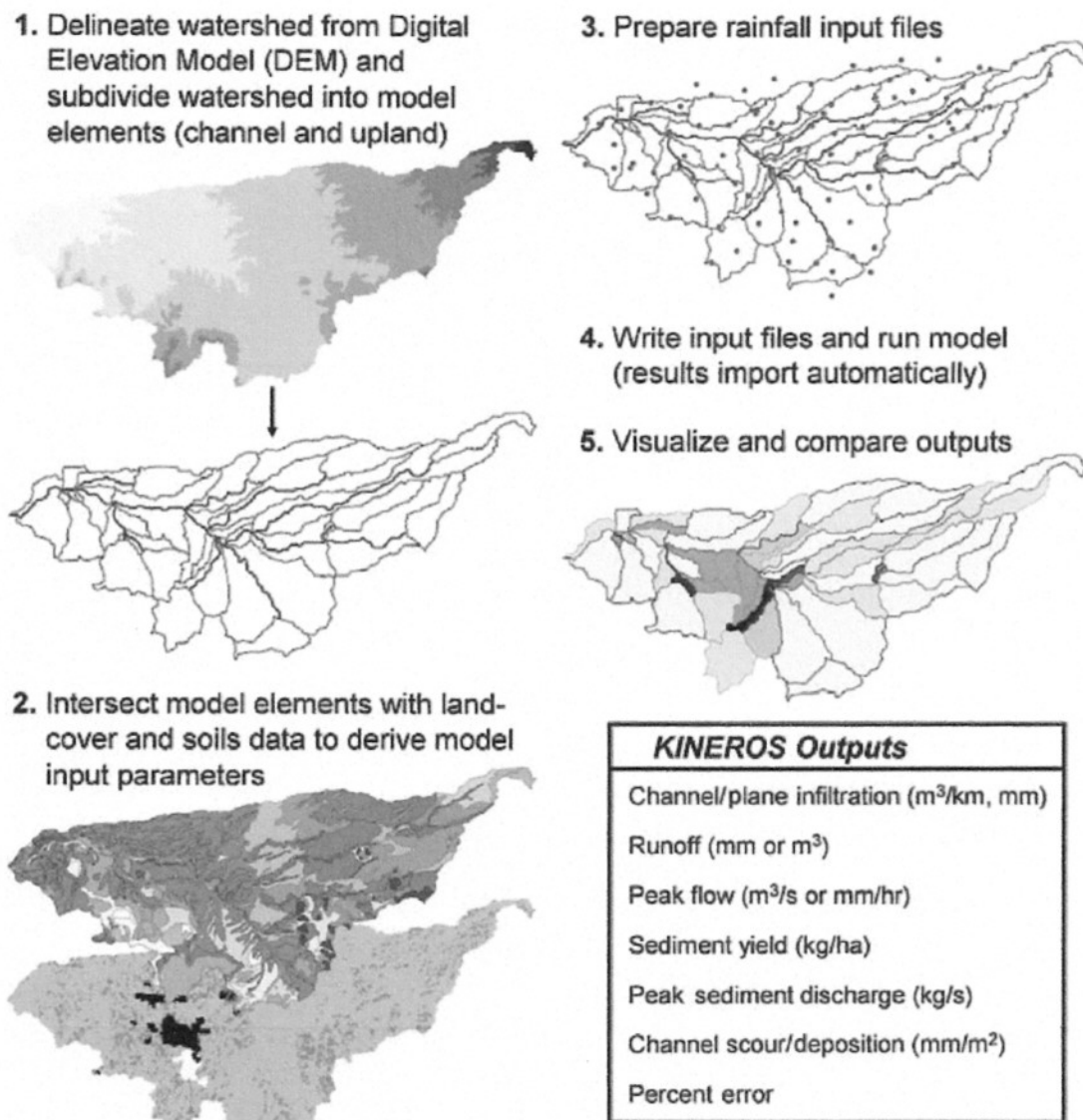


Figure 5.11 Sequence of steps in the use of KINEROS2 through AGWA

inter-disciplinary studies, scenario development, and alternative futures simulation work.

The following description of AGWA focuses on the K2 interface. Specifically, the interface design, processes, and ongoing research relating to the application of K2 are presented in detail. Miller *et al.* (2002) provide a more detailed description of AGWA-SWAT and its application in conjunction with K2 for multi-scale analyses. Hernandez *et al.* (2003) describe the integration of AGWA and ATtILA. Kepner *et al.* (2004) describe the use of AGWA for the analysis of alternative future land-use/cover scenarios, and the potential benefit to planning efforts. Burns *et al.* (2004) describe the development of a version of AGWA that was fully integrated into BASINS version 3.1.

5.3.2 Design

The conceptual design of AGWA is presented in Fig. 5.11. A fundamental assumption of AGWA is that the user has previously

compiled the necessary GIS data layers, all of which are easily obtained in most countries. The AGWA extension for ArcView adds the “AGWA Tools” menu to the View window, and must be run from an active view. Pre-processing of the DEM to ensure hydrologic connectivity within the study area is required, and tools are provided in AGWA to aid in this task. Once the user has compiled all relevant GIS data and initiated an AGWA session, the program is designed to lead the user in a stepwise fashion through the transformation of GIS data into simulation results. The AGWA Tools menu is designed to reflect the order of tasks necessary to conduct a watershed assessment, which is broken out into five major steps: (1) watershed delineation and subdivision; (2) land-cover and soils parameterization; (3) preparation of rainfall input files; (4) writing of input files and running of model; and (5) visualization and comparison of results.

Following model execution, AGWA will automatically import the model results and add them to the polygon and stream map-attribute tables for display. A separate module controls the

visualization of model results. Users can toggle among viewing various model outputs for both upland and channel elements, enabling the problem areas to be identified visually. If multiple land-cover scenes exist, they can be used to derive multiple parameter sets with which the models can be run for a given watershed. Model results can then be compared on either an absolute- or percent-change basis for each model element, and overlain with other digital data layers to help prioritize management activities.

5.3.2.1 WATERSHED DELINEATION AND SUBDIVISION

The most widely used method, and that which is used in AGWA, for the extraction of stream networks is to compute the accumulated area upslope of each pixel through a network of cell-to-cell drainage paths. This flow accumulation grid is subsequently pruned by eliminating all cells for which the accumulated flow area is less than a user-defined threshold drainage area, called the Channel, or Contributing Source Area (CSA). The watershed is then further subdivided into upland and channel elements as a function of the stream-network density. In this way, a user-defined CSA controls the spatial complexity of the watershed subdivision. This approach often results in a large number of spurious polygons and disconnected model elements. A suite of algorithms has been implemented in AGWA that refines the watershed elements by eliminating spurious elements and ensuring downstream connectivity.

Numerous options are available during the delineation and subdivision step that are designed to facilitate the application of K2 for real-world problems. Channel reaches and associated upland areas can be split at user-defined locations, such as flow gauges, to facilitate comparisons with observational data. Multiple watersheds can be delineated simultaneously to accommodate areas of concern not falling neatly within watershed boundaries, such as governmental jurisdictions. Ponds (releasing or non-releasing) and riparian buffer strips can also be incorporated during the subdivision process.

5.3.2.2 PARAMETER ESTIMATION

Each of the overland and channel elements delineated by AGWA is represented in K2 by a set of parameter values. These values are assumed to be uniform within a given element. There may be a large degree of spatial variability in the topographic, soil, and land-cover characteristics within the watershed, and AGWA uses an area-weighting scheme to determine an average value for each parameter within an overland flow model element abstracted to an overland flow plane (Miller *et al.*, 2002). GIS layers are intersected with the subdivided watershed, and a series of look-up tables and spatial analyses are used to estimate parameter values

for the unique combinations of land cover and soils. K2 requires a host of parameter values, and estimating their values can be a tedious task; AGWA rapidly provides estimates based on an extensive literature review and calibration efforts. This convenience does not obviate the need for calibrating K2 applications, and uncalibrated model results should thus be used only in qualitative assessments. Users are able to modify input parameters by adjusting values in the provided look-up tables prior to running the land-cover and soils parameterization, or by adjusting the parameters associated with each element following the parameterization.

Soil parameters for upland elements as required by K2 (such as percent rock, suction head, porosity, saturated hydraulic conductivity) are initially estimated from soil texture according to the soil data following Woolhiser *et al.* (1990) and Rawls *et al.* (1982). Saturated hydraulic conductivity is reduced following Bouwer (1966) to account for air entrapment. Further adjustments are made following Stone *et al.* (1992) as a function of estimated canopy cover, and following Bouwer and Rice (1984) as a function of the amount of rock fragments in the soil. Area and depth weighting procedures are used to derive a single representative soil profile for each upland element. Cover parameters, including interception, canopy cover, Manning's roughness, and % paved area are estimated following expert opinion and previously published look-up tables (Woolhiser *et al.*, 1990). Upland element slope is estimated as the average slope within the element, and width and length are a function of the element shape, which is assumed to be rectangular with element length equal to longest flow length. Stream-channel slope is estimated as the difference in elevation between the reach endpoints divided by the reach length. Channel width and depth are parameterized using regional hydraulic-geometry relationships, or regression equations relating contributing area to channel dimensions (e.g., Miller *et al.*, 1996). An editable database of published hydraulic-geometry relationships is provided with AGWA, or custom relationships can be specified by the user. AGWA is unable to derive soil-related parameters for channels from GIS data and therefore assumes that all channels have a sandy bed. These parameters can be easily edited through the stream-reach attribute table if necessary.

Digital soil maps for different countries or regions vary considerably in terms of the information they contain, and how that information is organized in their associated database files. Automated use of soil maps for model parameterization is heavily dependent on this information structure, and thus not just any soil map can be used with AGWA. As a result, procedures to use the United Nations Food and Agriculture Organization's (FAO) Digital Soil Map of the World were developed to maximize the geographic extent of its applicability. Despite the relatively low spatial resolution of the FAO soil maps, K2 results derived using them compare well with results derived from higher resolution soil maps in the United States (Levick *et al.*, 2004; Levick *et al.*, 2006).

5.3.2.3 RAINFALL INPUT

Uniform rainfall input files for K2 can be created in AGWA using gridded return-period rainfall maps, a database of geographically specific return-period rainfall depths provided with the tool, or using data entered by the user. Return-period rainfall depths are converted to hyetographs using USDA Soil Conservation Service (SCS) methodology and a type-II distribution (USDA-SCS, 1973). The hypothetical type-II distribution is suitable for deriving the time distribution of 24-hour rainfall for extreme events in many regions, but may result in overestimated peak flows, particularly when applied to shorter-duration events.

If return-period rainfall grids are available, then AGWA extracts the rainfall depth for the grid cell containing the centroid of the watershed for which the rainfall input file is being generated. The depth is then converted into a hyetograph for the specified return period using the SCS methodology described above. This process has been automated for convenient use with common datasets available in the United States, and can be easily modified to accommodate other formats.

If return-period rainfall maps are not available, or a specific depth and duration are desired, the provided design-storm database file can be easily edited to add new data. Data are entered in the form of a location, recurrence interval, duration, and rainfall depth in millimeters. The design-storm database further provides the option to incorporate an area-reduction factor, if known, which can be particularly convenient when working in regions characterized by convective thunderstorms.

In the event that gauge observations of rainfall depth are available, or a specific hyetograph is desired, then data may be entered manually by the user through the AGWA interface. User-defined storms are entered as time-depth pairs, thus providing the flexibility to define any hyetograph.

Version 1.5 of AGWA also incorporates the ability to create distributed rainfall input files for K2. This feature allows users to select the gauges, include gauges with zero depths for more accurate interpolation by K2, set a minimum depth that the gauges must exceed before creating a rainfall file, and generate files for any number of events between a given range of dates.

5.3.2.4 MODELLING

Once model element parameters have been assembled and a rainfall input file has been written, AGWA can write the K2 parameter file and run the model. When this option is selected the user is presented with the opportunity to enter parameter multipliers for the most sensitive channel and upland parameters. Multipliers, which default to 1.0, are entered as real numbers and can be used to manipulate parameters as they are written to the parameter file. This option is particularly useful during calibration and sensitivity exercises. Parameter files generated or modified outside of AGWA may also be run through the AGWA interface, provided that they

correspond with an existing watershed configuration within the AGWA project.

Once parameter files are written or selected, K2 is called automatically and runs in a separate command window. When the simulation is complete, AGWA reads the output file and results for each model element are parsed back into an ArcView database file, which is stored in the AGWA project and available for viewing.

5.3.2.5 RESULTS VISUALIZATION AND COMPARISON

Simulation results can be selected and viewed using the AGWA visualization tool. When selected, results database files are joined with the polygon and stream map-attribute tables to associate output for each model element with its corresponding polygon or line on the map. Once selected from a list of available outputs, results are automatically divided into nine equal-interval classes and mapped with graduated colors to provide users with the ability to rapidly assess the spatial variability of results within the watershed.

Results may also be easily compared for multiple simulations in the same watershed by computing differences in terms of absolute values or percentages. Differences are written to a new database file that is treated as a separate simulation result and available for visualization. Common comparisons, or relative assessments, include results from simulations based on different land-use/cover conditions, which may represent historic observations or projected future conditions. This option makes it possible to rapidly evaluate the spatial patterns of hydrologic response to landscape change, and to target mitigation and restoration activities for maximum effect.

5.3.3 Scenario building

The use of AGWA as a strategic planning tool has been accommodated through the addition of a land-cover modification tool that allows users to manipulate land-cover grids to represent alternative future land-use/cover scenarios. Changes are carried out within polygons that can be interactively drawn on the screen or taken from imported shapefiles. A variety of types of change can be prescribed, including:

- (1) Change entire area to a new land-cover type (e.g., to urban).
- (2) Change one land-cover type to another within a user-defined area (e.g., to simulate unpaved road restoration, change barren to desert scrub).
- (3) Create a random land-cover pattern (e.g., to represent a burn pattern, change to 64 % barren, 31 % desert scrub, and 5 % mesquite woodland). Patterns can be completely spatially

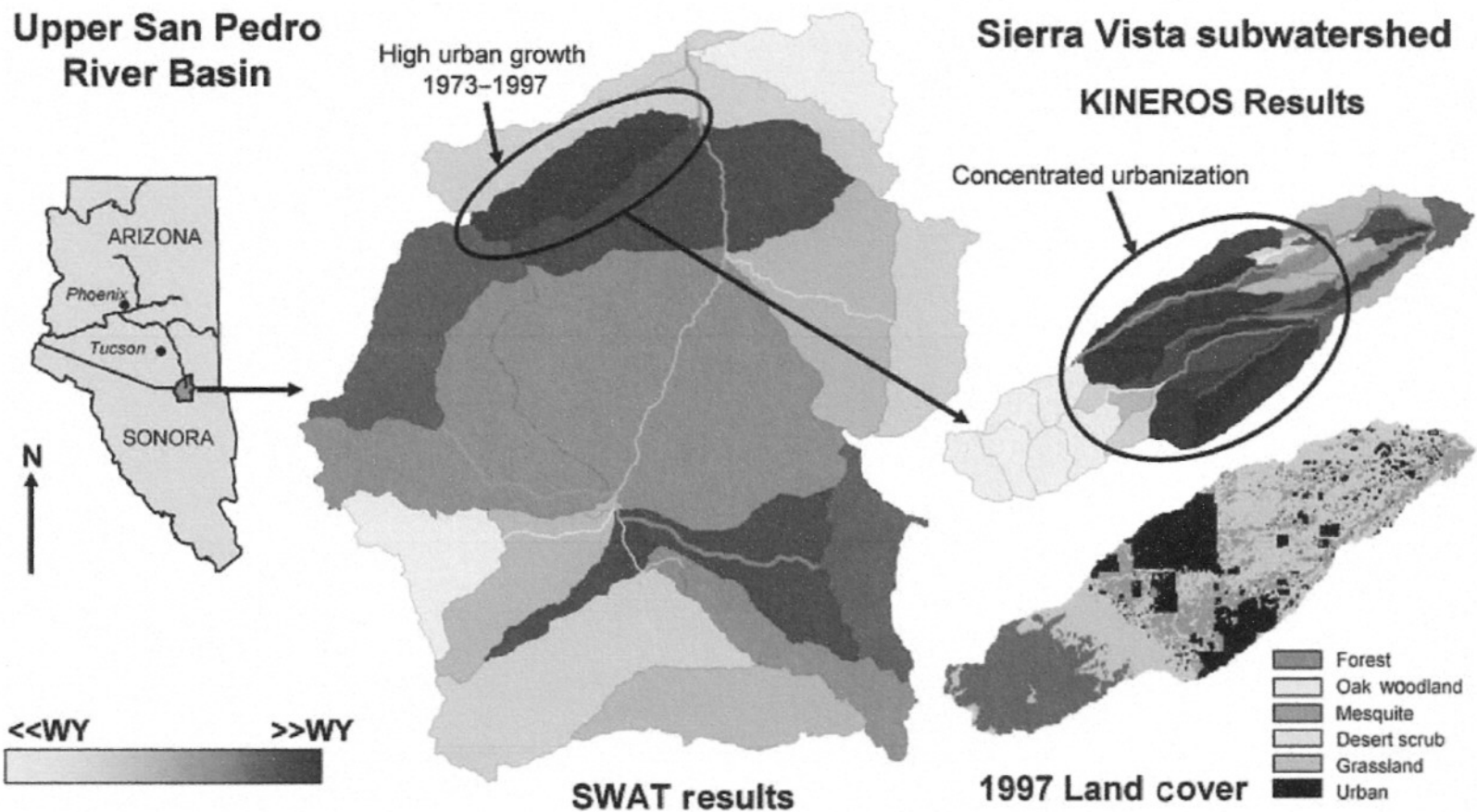


Figure 5.12 Model results from the upper San Pedro River Basin and Sierra Vista subwatershed showing the relative increase in simulated water yield as a result of urbanization between 1973 and 1997. Also demonstrated is the multi-scale assessment capability of AGWA; basin-scale effects observed with SWAT can be investigated at the small-watershed scale with KINEROS2

random or multifractal randomly distributed patchy, with patch size (degree of clustering) controlled by the user.

(4) Modify a land-cover grid based on a burn-severity map.

Using the land-cover modification tool in combination with the relative assessment functionality described in the previous section, it is possible to build a suite of alternative future scenarios and evaluate their relative merits in terms of impact to the local hydrology.

5.3.4 Example application: upper San Pedro River multi-scale assessment

Flowing north from Sonora, Mexico into southeastern Arizona, the San Pedro River Basin has a wide variety of topographic, hydrologic, cultural, and political characteristics. The basin is an exceptional example of desert biodiversity in the semi-arid southwestern United States, and a unique study area for addressing a range of scientific and management issues. It is also a region in socioeconomic transition as the previously dominant rural ranching economy is shifting to increasing areas of urban development. The area is a transition zone between the Chihuahuan and Sonoran

deserts and has a highly variable climate with significant biodiversity. The tested watershed is approximately 3150 km² and is dominated by desert shrub-steppe, riparian, grasslands, agriculture, oak and mesquite woodlands, and pine forests.

The AGWA tool was used to delineate the upper San Pedro above the USGS Charleston gauge, and prepare input parameter files for SWAT. The watershed was subdivided using the AGWA default CSA value of 2.5 % of the total watershed area, or approximately 79 km². Parameter files were built using both the 1973 and 1997 Landsat satellite classified land-cover scenes. SWAT was run for each of these using the same ten years of observed daily precipitation and temperature data for a single location. By using the same rainfall and temperature inputs, simulated changes in water yield are due solely to altered land cover within the watershed. The “differencing” feature in AGWA was used to compute the % change between the two simulation results and display it visually (Fig. 5.12). This analysis showed that a small watershed running through the developing city of Sierra Vista, shown in Fig. 5.12 as the “Sierra Vista subwatershed,” underwent changes in its land cover that profoundly affected the hydrologic regime.

The Sierra Vista subwatershed (92 km²) was modelled in greater detail using K2. It was also subdivided using a CSA value of 2.5 %,

and run using both the 1973 and 1997 land-cover data. A uniform design storm representing the 10-year, 60-minute event (Osborn *et al.*, 1985) was used in both simulations. Since applying point estimates for design storms across larger areas tends to lead to the over-prediction of runoff due to the lack of spatial heterogeneity in input data, an area-reduction method developed by Osborn *et al.* (1980) is used in AGWA to reduce rainfall estimates for watersheds in the San Pedro Basin. Percent change in runoff between the two simulations was computed using the “differencing” tool in AGWA, and the results are presented (directly from AGWA) in Fig. 5.12. From this analysis it is clear that the hydrologic response of the region of concentrated urban growth is adequately represented. Increasing impervious area associated with urban growth has resulted in large increases in runoff from those areas where urbanization is highest.

This type of relative-change assessment is considered to be the most effective use of the AGWA tool without calibrating its component models for a particular site. Without calibration, absolute values of model output parameters should not be considered accurate, nor should the magnitude of computed changes. In a relative sense, however, AGWA can still be useful for inexpensively identifying locations in ungauged watersheds that are particularly vulnerable to degradation, and where restoration activities may therefore be most effective. The ability to use a second model to zoom in on sensitive areas provides a further means of focusing restoration efforts, or preventative measures if the tool is being used to assess potential future scenarios.

5.4 RESEARCH AND DEVELOPMENT

5.4.1 KINEROS2

K2 is a Fortran 77 code designed to handle an unlimited number of model elements (planes, channels, etc.) while keeping the compiled program size under the 640 KB limit imposed by the original MS-DOS operating system. The memory-efficient design features of K2 served it well during the early period of personal computing. At the present time, however, there is tremendous processing power and huge memory resources available on personal computers, both in hardware and through the use of virtual memory strategies like page file swapping. Therefore the hardware and operating system issues that K2 was designed to address no longer exist. Fortran itself has also advanced to a new standard, Fortran 90/95. Fortran 90/95 provides dynamic memory allocation, a proprietary pointer mechanism and modules that encapsulate data structures and procedures, allowing a rudimentary object-oriented programming approach. Also, although K2 is composed of well-defined components, those components were designed to be parts of a

whole and not to function independently. This monolithic nature of K2 has led to a number of modified versions, each of which must be maintained as a separate program.

To overcome the design limitations of K2, and to take advantage of features offered by Fortran 90/95, the K2 code was deconstructed and rebuilt into a library of Fortran 90/95 modules, with each module implementing a single process model, or object (Goodrich *et al.*, 2006). Two major goals of this restructuring are to make K2 technology more readily available to developers of new programs that could benefit from its capabilities, and to make versions of K2 that have been modified for specialized applications easier to maintain. In the restructured version of K2 each object is controlled through an interface, or set of procedures, that are designed to simplify use of the object by non-Fortran programs. This is desirable in that none of the popular and full-featured graphical user interface development products are based on Fortran.

The new structure makes it possible to iterate over all elements at each time-step, rather than each element over all time-steps, as is done by K2. Examples would be open-ended simulations, such as real-time operation, or to graphically display the spatial distribution of simulated quantities, such as runoff from each element, at each time-step during a simulation. In addition to the core process models, there are utility modules to conveniently support backward-compatibility, such as one to extract parameters from a K2 input file. Compatibility between future versions of the module library is also ensured by not allowing existing procedures to be removed, or their names or argument lists to change, although they can change internally. Additional procedures that support extensions to a module’s capabilities can be added in the future as long as suitable defaults can allow existing programs to use the module without calling the procedures.

5.4.2 AGWA

A number of ongoing research projects are designed to develop and evaluate strategies for improving the accuracy and usability of K2 through the AGWA interface. These will ultimately be implemented as new tools that will be available to AGWA users, so they are summarized here to provide the reader with an idea of how AGWA will be enhanced in the near future.

Improvements to the accuracy of K2 simulations developed through the AGWA interface are focused on improving its ability to utilize remotely sensed data, including new sources that are becoming increasingly available. One such project is evaluating the potential to improve the watershed subdivision procedure by utilizing additional information available on topographic, land-cover, and soil maps. The goal of this effort is to improve the automated recognition of hydrologic response units in terms of

slope, cover, and soil type so that they may be split out during the subdivision process and thus minimize intra-element parameter variability.

Radar rainfall data is another source of remotely sensed data that is becoming more popular as a source of data for hydrologic models (e.g., Morin *et al.*, 2003). A project currently underway is evaluating the potential to utilize this data in real time for the purpose of predicting flash flooding in arid regions. A customized version of AGWA has been developed to read in level II NEXRAD 1 km \times 1° radar images at five-minute intervals, and process that information for distributed input to the restructured version of K2, which can be run one time-step at a time.

Airborne Light Detection and Ranging (LIDAR) data is another type of remotely sensed data that holds a large potential benefit to GIS-based hydrologic modelling. It provides high-resolution (\sim 1 m) topographic information that can improve channel characterization. AGWA currently uses simple hydraulic-geometry relationships to estimate channel dimensions because they cannot be resolved from typical DEM data (Miller *et al.*, 2004). With LIDAR data, however, it is possible to derive detailed channel morphologic information, and a tool is being developed to extract it for the purpose of reach-based characterization (Semmens *et al.*, 2006) as needed by K2 and numerous other models.

Other planned improvements to the AGWA interface focus on providing users with tools to support environmental management and planning. Scenario development is a key component of this work, and is being approached from three different perspectives: climate, land-cover/use, and management activities. A climatic-scenario generator will permit the development of prescribed climate changes and evaluation of their associated impacts given current or anticipated future management conditions. A new modelling tool will permit the simulation of large-scale changes in land-cover/use, in addition to the prescribed changes already possible through the land-cover modification tool, for the evaluation of different spatial patterns of potential landscape change. A best management practice (BMP) tool will allow users to modify land-cover surfaces based on defined plant transitions and the management practices driving them (Scott, 2005). Finally, the functionality to parameterize the K2 urban element feature is presently under development and will permit the rapid evaluation of alternative impervious-surface management strategies.

5.4.2.1 THE NEXT GENERATION OF AGWA

The final version of AGWA for ArcView 3.X, version 1.5, was released in early 2006. This software will continue to be maintained, but research and development will be focused on two new versions of AGWA: one for ArcGIS 9.X (AGWA 2.0), and one for the Internet (DotAGWA). AGWA 2.0 and DotAGWA, due for Beta release in 2006 and 2007, respectively, will incorporate the

same functionality as AGWA 1.5, but are designed to meet several additional criteria: (1) maximize the capacity to incorporate additional models, including non-hydrologic models, (2) facilitate the interaction between observed and modelled information at multiple scales, and (3) maximize potential user audiences.

AGWA 2.0 will be distributed as a custom tool for ArcGIS 9.X that can be loaded to ArcMap. It will include greater flexibility to incorporate user-provided/defined information, additional tools for scenario development and the analysis and visualization of model results, and improved watershed subdivision and parameterization functionality to enhance the performance and application of K2. AGWA 2.0 will provide the maximum flexibility to work with input provided by the user and to manipulate the parameters and settings of K2 simulations, thus facilitating model calibration.

DotAGWA is designed to assist in the decision-making processes by making AGWA functionality available to a much larger audience, namely those without access to proprietary GIS software and/or the GIS skills needed to assemble necessary input datasets (Cate *et al.*, 2005; Cate *et al.*, 2006). The DotAGWA design includes features that will help users share and visualize data by providing access to the application through an Internet browser interface. Different stakeholder groups will be able to interact with the application to help facilitate the communication and decision-making processes. Users will be able to define management scenarios, attach models to a plan, and have the application parameterize and run the models for the defined management plan. Multiple file-format options (e.g., text, XML, and HTML) will be available for exporting simulation outputs.

5.4.3 AGWA-KINEROS

Rather than running K2 as an external program, future versions of AGWA 2.0 and DotAGWA will be able to utilize the restructured K2 object library to enhance interaction between model and GIS interface. This will open up many possibilities by giving AGWA access to complete information about every element at each time step. For example, AGWA could animate the spatial development of runoff, infiltration or sediment production during a simulation. The user could have control over the animation speed, pause progress, change which quantities are displayed, or terminate the simulation at any time. Breakpoints could be set to pause the simulation at predetermined times, and it would be possible to "rewind" the simulation back to a previous breakpoint. Additional windows could monitor the longitudinal profile of the water surface in channels, as well as sediment concentration and bed deposition and scour. Using the object library would also make it easier to expand the sources of input data, such as radar rainfall and LIDAR topographic data.

5.5 REFERENCES

- Arnold, J. G., J. R. Williams, and D. A. Maidment. (1995). A continuous time water and sediment routing model for large basins. *J. Hydr. Eng.*, **121** (2), 171–83.
- Bennett, J. P. (1974). Concepts of mathematical modeling of sediment yield. *Water Resour. Res.*, **10** (3), 485–92.
- Bingner, R. L. and Theurer, F. D. (2001). AGNPS 98: A suite of water quality models for watershed use. *Proceedings of the 7th Federal Interagency Sedimentation Conference*, Reno, NV, March 25–29, 2001, VII–1–VII–8.
- Bouwer, H. and Rice, R. C. (1984). Hydraulic properties of stony vadose zones. *Groundwater*, **22** (6), 696–705.
- Bouwer, H. (1966). Rapid field measurement of air entry and hydraulic conductivity as significant parameters in flow systems analysis. *Water Resour. Res.*, **2**, 729–38.
- Burns, I. S., Semmens, D. J., Scott, S. N., Levick, L. R., Goodrich, D. C., and Kepner, W. G. (2004). The Automated Geospatial Watershed Assessment (AGWA) tool – enhanced capabilities of just released version 1.4. *Proceedings of the Arizona Hydrological Society 17th Annual Symposium*, Sept. 5–18, Tucson, AZ.
- Cate, A. J. Jr., Semmens, D. J., Burns, I. S., Goodrich, D. C., and Kepner, W. G. (2005). *AGWA Design Documentation: Migrating to ArcGIS and the Internet*. US EPA Report EPA/600/R-05/056, USDA-ARS Report ARS/181027.
- Cate, A. Jr., Goodrich, D. C., and Guertin, D. P. (2006). Integrating hydrologic models and spatial data in a distributed Internet application. *Proceedings of the Third Federal Interagency Hydrologic Modeling Conference*, April 3–6, 2006, Reno, NV (<http://www.tucson.ars.ag.gov/unit/publications/pdffiles/1801.pdf>).
- Corradini, C., Melone, F., and Smith, R. E. (2000). Modeling local infiltration for a two-layered soil under complex rainfall patterns. *J. Hydrol.*, **237** (1–2), 58–73.
- Ebert, D. W. and Wade, T. G. (2004). *Analytical Tools Interface for Landscape Assessments (ATiLA) Version 2004 User Manual*. US EPA Report EPA/600/R-04/083.
- Engelund, F. and Hansen, E. (1967). *A Monograph on Sediment Transport in Alluvial Streams*. Copenhagen: Teknisk Forlag.
- ESRI (2001). *ArcView Version 3.2a Software and User Manual*. Redlands: Environmental Systems Research Institute.
- Fair, G. M. and Geyer J. C. (1954). *Water Supply and Wastewater Disposal*. New York: Wiley.
- Goodrich, D. C., Unkrich, C. L., Smith, R. E., and Woolhiser, D. A. (2002). KINEROS2 – a distributed kinematic runoff and erosion model. *Proceedings of the Second Federal Interagency Hydrologic Modeling Conference*, July 29–Aug. 1, Las Vegas, NV.
- Goodrich, D. C., Unkrich, C. L., Smith, R. E., and Woolhiser, D. A. (2006). KINEROS2 – new features and capabilities. *Proceedings of the Third Federal Interagency Hydrologic Modeling Conference*, April 3–6, 2006, Reno, NV (http://www.tucson.ars.ag.gov/unit/publications/pdf_files/1799.pdf).
- Green, W. H. and Ampt, G. (1911). Studies of soil physics. Part I: The flow of air and water through soils. *J. Agri. Sci.*, **4**, 1–24.
- Hernandez, M., Kepner, W. G., Semmens, D. J., et al. (2003). Integrating a landscape/hydrologic analysis for watershed assessment. *Proceedings of the First Interagency Conference on Research in the Watersheds*, Benson, AZ, Oct 27–30. USDA, Agricultural Research Service, 461–466.
- Kepner, W. G., Semmens, D. J., Basset, S. D., Mouat, D. A., and Goodrich, D. C. (2004). Scenario analysis for the San Pedro River, analyzing hydrological consequences for a future environment. *Environ. Mod. Assess.*, **94**, 115–27.
- Lahlou, M., Shoemaker, L., Choudry, S., et al. (1998). *Better Assessment Science Integrating Point and Nonpoint Sources: BASINS 2.0 User's Manual*. US EPA Report EPA-823-B-98–006.
- Levick, L. R., Semmens, D. J., Guertin, D. P., et al. (2004). Adding global soils data to the Automated Geospatial Watershed Assessment tool (AGWA). *Proceedings of the Second International Symposium on Transboundary Waters Management*, Nov 16–19, Tucson, AZ.
- Levick, L. R., Guertin, D. P., Scott, S. N., Semmens, D. J., and Goodrich, D. C. (2006). Automated Geospatial Watershed Assessment tool (AGWA): uncertainty analysis of common input data. *Proceedings of the Third Federal Interagency Hydrologic Modeling Conference*, April 3–6, Reno, NV. (<http://www.tucson.ars.ag.gov/unit/publications/pdffiles/1797.pdf>)
- Meyer, L. D. and Wischmeier, W. H. (1969). Mathematical simulation of the process of soil erosion by water. *Trans. Am. Soc. Agri. Eng.*, **12** (6), 754–62.
- Miller, S. N., Guertin, D. P., and Goodrich, D. C. (1996). Linking GIS and geomorphology field research at Walnut Gulch. *Proceedings of the American Water Resources Association 32nd Annual Conference and Symposium: "GIS and Water Resources"*, Sept. 22–26, Ft. Lauderdale, FL, 327–35.
- Miller, S. N., Semmens, D. J., Miller, R. C., et al. (2002). GIS-based hydrologic modeling: The Automated Geospatial Watershed Assessment tool. *Proceedings of the Second Federal Interagency Hydrologic Modeling Conference*, July 29–Aug 1, Las Vegas, NV.
- Miller, S. N., Shrestha, S. R., and Semmens, D. J. (2004). Semi-automated extraction and validation of channel morphology from LIDAR and IFSAR terrain data. *Proceedings of the 2004 American Society for Photogrammetry and Remote Sensing Annual Conference*, May 23–28, Denver, CO.
- Morin, E., Krajewski, W. F., Goodrich, D. C., Gao, X., and Sorooshian, S. (2003). Estimating rainfall intensities from weather radar data: the scale-dependency problem. *J. Hydrometeorol.*, **4**, 782–97.
- Morris, E. M. and Woolhiser, D. A. (1980). Unsteady one-dimensional flow over a plane: partial equilibrium and recession hydrographs. *Water Resour. Res.*, **16** (2), 355–60.
- Osborn, H. B., Lane, L. J., and Myers, V. A. (1980). Rainfall/watershed relationships for southwestern thunderstorms. *Trans. Am. Soc. Civ. Eng.*, **23** (1), 82–91.
- Osborn, H. B., Unkrich, C. L., and Frykman, L. (1985). Problems of simplification in hydrologic modeling. *Hydrology and Water Resources in Arizona and the Southwest, Arizona-Nevada Academy of Science*, **15**, 7–20.
- Parlange, J.-Y., Lisle, I., Braddock, R. D., and Smith, R. E. (1982). The three-parameter infiltration equation. *Soil Sci.*, **133** (6), 337–41.
- Rawls, W. J., Brakensiek, D. L., and Saxton, K. E. (1982). Estimation of soil water properties. *Trans. Am. Soc. Agri. Eng.*, **25** (5), 1316–20, 1328.
- Reeves, M. and Miller, E. E. (1975). Estimating infiltration for erratic rainfall. *Water Resour. Res.*, **11** (1), 102–10.
- Rovey, E. W. (1974). A kinematic model for upland watersheds. Unpublished M.Sc. thesis, Colorado State University, Fort Collins.
- Rovey, E. W., Woolhiser, D. A., and Smith, R. E. (1977). *A Distributed Kinematic Model for Upland Watersheds*. Hydrology Paper No. 93, Colorado State University.
- Scott, S. (2005). Implementing best management practices in hydrologic modeling using KINEROS2 and the Automated Geospatial Watershed Assessment (AGWA) tool. Unpublished M.Sc. thesis, University of Arizona, Tucson.
- Semmens, D. J., Miller, S. N. and Goodrich, D. C. (2006). Towards an automated tool for channel-network characterization, modeling and assessment. *Proceedings of the Third Federal Interagency Hydrologic Modeling Conference*, April 3–6, Reno, NV. (<http://www.tucson.ars.ag.gov/unit/publications/pdffiles/1800.pdf>)
- Smith, R. E. (1990). Analysis of infiltration through a two-layer soil profile. *Soil Sci. Soc. Am. J.*, **54** (5), 1219–27.
- Smith, R. E. and Goodrich, D. C. (2000). Model for rainfall excess patterns on randomly heterogeneous areas. *J. Hydrol. Eng.*, **5** (4), 355–62.
- Smith, R. E. and Parlange, J.-Y. (1978). A parameter-efficient hydrologic infiltration model. *Water Resour. Res.*, **14** (3), 533–8.
- Smith, R. E., Corradini, C., and Melone, F. (1993). Modeling infiltration for multistorm runoff events. *Water Resour. Res.*, **29** (1), 133–44.
- Smith, R. E., Goodrich, D. C., and Quinton, J. N. (1995b). Dynamic, distributed simulation of watershed erosion: the KINEROS2 and EUROSEM models. *J. Soil Water Conserv.*, **50**(5), 517–20.
- Smith, R. E., Goodrich, D. C., Woolhiser, D. A., and Unkrich, C. L. (1995a). KINEROS – a kinematic runoff and erosion model. In *Computer Models of Watershed Hydrology*, ed. V. J. Singh, Highlands Ranch, CO: Water Resources Publications, 697–732.
- Smith, R. E., Smettem, K. R. J., Broadbridge, P., and Woolhiser, D. A. (2002). *Infiltration Theory for Hydrologic Applications*. Water Resources Monograph Series, Vol. 15. Washington, DC: American Geophysical Union.
- Stone, J. J., Lane, L. J., and Shirley, E. D. (1992). Infiltration and runoff simulation on a plane. *Trans. Am. Soc. Agri. Eng.*, **35** (1), 161–70.
- Unkrich, C. L. and Osborn, H. B. (1987). Apparent abstraction rates in ephemeral stream channels. *Hydrology and Water Resources in Arizona and the Southwest, Arizona-Nevada Academy of Science*, **17**, 34–41.

- USACE (2003). *Geospatial Hydrologic Modeling Extension: HEC-GeoHMS User's Manual*. US Army Corps of Engineers, Hydrologic Engineering Center, Report CPD-77.
- USDA-SCS. (1973). *A Method for Estimating Volume and Rate of Runoff in Small Watersheds*. SCS-TP-149. Washington, DC: US Department of Agriculture, Soil Conservation Service.
- Wilgoose, G. and Kuczera, G. (1995). Estimation of subgrid scale kinematic wave parameters for hillslopes. In *Scale Issues in Hydrologic Modeling*, ed. J. D. Kalma and M. Sivapalan, Chichester: John Wiley & Sons, pp. 227–240.
- Woolhiser, D. A. and Liggett, J. A. (1967). Unsteady, one-dimensional flow over a plane – the rising hydrograph. *Water Resour. Res.*, **3** (3), 753–71.
- Woolhiser, D. A., Hanson, C. L., and Kuhlman, A. R. (1970). Overland flow on rangeland watersheds. *J. Hydrol. (New Zealand)*, **9** (2), 336–56.
- Woolhiser, D. A., Smith, R. E., and Goodrich, D. C. (1990). *KINEROS, A Kinematic Runoff and Erosion Model: Documentation and User Manual*. US Department of Agriculture, Agricultural Research Service, ARS-77.
- Woolhiser, D. A., Smith, R. E., and Giraldez, J.-V. (1997). Effects of spatial variability of saturated hydraulic conductivity on Hortonian overland flow. *Water Resour. Res.*, **32** (3), 671–8.